Research Article

Finite Element Investigation of Angle Ring Confinement for Clustered Large-size Stud Shear Connector in Full-Depth Precast Concrete Bridge Deck Panel

Krissachai Sriboonma* and Chichaya Boonmee
Department of Teacher Training in Civil Engineering, Faculty of Technical Education, King Mongkut's University of Technology North Bangkok, Bangkok, Thailand

Sacharuck Pornpeerakeat
Department of Teacher Training in Civil Engineering, Faculty of Technical Education, King Mongkut's University of Technology North Bangkok, Bangkok, Thailand
Research Centre for Advanced Computational and Experimental Mechanics (RACE), King Mongkut's University of Technology North Bangkok, Bangkok, Thailand

Kittipoom Rodsin
Civil and Environmental Engineering Technology, College of Industrial Technology, King Mongkut's University of Technology North Bangkok, Bangkok, Thailand

Natawut Chaiwino
Department of Technical Education, Faculty of Technical Education, Rajamangala University of Technology Thanyaburi, Phatum Thani, Thailand

Abstract
Full-Depth Precast Concrete (FDPC) bridge deck panel system, consisting of concrete deck and steel girders, has been used widely for highway and bridge construction due to rapid construction and replacement as well as in terms of economics. This system could integrate with clusters of large size headed-stud shear connectors for more significant connection, although larger composite actions were experienced. Therefore, a new angle steel ring confinement was introduced and tested by push-off samples for the most effective shear transfer. The Finite Element Analysis (FEA) of the push-off model with an in-depth investigation of non-linear concrete properties, boundary parameters, and different geometries of angle ring confinement was developed in this study. The FE models were verified with the push-off test in terms of loads, displacements, and failure stages. Non-linear concrete material models: Concrete Damage (CD) and Drucker Prager (DP) were identified the different abilities either for predicting initial cracks, or determining maximum resistance and critical failure, respectively. The thickness of the angle and the sizes of hook bars were investigated for the most effective aspects of the angle ring confinement. The results showed comparable stiffness and load resistance for various aspects. However, compatible geometries, either 5 mm thick angles with DB12 hook bars or 10 mm angles with DB25 hook bars, were suggested. The final non-linear FEA model was reliable for comparative studies to FDPC push-off with different confinement configurations.

Keywords: Finite element, Angle ring confinement, Shear pocket, Full-depth precast concrete, Large-size stud

1   Introduction

Full-depth precast concrete (FDPC) bridge deck panel systems have been developed since the 1990s [1] and widely used for highway and bridge construction due to timesaving for new or replacing of precast concrete decks with steel girders. Connections of this system are typically provided by using stud shear connectors to create composite actions and shear transfer between the interfaces. Composite actions, in terms of lateral shear forces, are expected to fully develop, which are important to the system especially when using headed-stud shear connectors. According to AASHTO LRFD specification [2] maximum spacing of adjacent studs was suggested up to 600 mm (24 in).

To significantly improve the construction process, the systems were integrated with novel connections using 1) large-size stud shear connectors and 2) stud clusters instead of line spaced studs. A cluster of studs could implement with a group of 2, 4 or even 8 studs for a typical diameter of 19 mm (¾ in) studs, while the spacing between each cluster consisted of 600 mm (24 in) per AASHTO LRFD guideline. The study of Badie *et al.* [3], [4] revealed that the full-scale test of the composite bridge deck system with clusters of large-size diameter studs of 31.8 mm (1¼ in) could extend the spacing of clusters up to 1200 mm (48 in). This could effectively transfer the composite actions under the service loading condition. However, shear transferring forces could not be fully developed as much as twice of the spacing during the ultimate loading. The initial cracks were observed around the concrete shear pocket and the confinement of the stud cluster. The early cracks caused non-fully composite actions per AASHTO LRFD resistance equations.

Sriboonma *et al.* [5] explained the practical guideline for using large size stud shear connectors in full-depth precast bridge deck panel to efficiently carry the composite actions and shear transfers. Several push-off tests of a cluster of large size studs with different types of steel confinement were investigated under static and cyclic loading [6], [7]. The results under static loading showed that the specimens with a cluster of 8-large size studs could resist higher shear force about 50–100% than those with a cluster of 4-large size shear studs. Relatively, higher relative displacements of about 20–50% were observed for the specimens with a cluster of 8-large size studs

(higher ductility). In terms of failure, initial hairline cracks were also noticed at the bottom of the concrete deck and then propagated around the side of the deck. Cracks also spread out around the shear pocket and/or tearing of steel confinements (on the bearing face around the shear pocket) were detected in most of the specimens regardless of different types of confinement. The steel angle ring confinement could gain the highest shear resistance and greatest ductility. Therefore, this type of steel confinement was implemented for a comparative study to FEA in this research as will be explained in the next section.

On the other hand, the experiment under cyclic loading found that fatigue resistance equations per AASHTO LRFD specification Article 6.10.10.2 based on a single shear stud governed for designing a cluster of large-size studs under the failure mode of the concrete deck [7]. This included the modified steel angle confinement with hook bars to achieve the fatigue resistance limit. No permanent deformation of the steel angle was detected under the initial cracking stage of concrete. Hook bars also helped attach the concrete deck and shear pocket in place as well as increasing ductility, stiffness and effectiveness of composite actions to the panel.

Other methods to increase the speed of construction to the FDPC system were introduced recently involving modification of material properties, aspect ratio of shear pocket, confinement, thickness of deck, and height of studs. Fang *et al.* [8] evaluated various aspect ratios among diameter/height of studs to the depth and thickness of FDPC systems using Ultra-High-Performance-Concrete (UHPC). The studies presented in terms of load resistance, shear stiffness, load-slip prediction for group short bolts embedded in thin full-depth UHPC slabs. Wang *et al.* [9] has also studied the static behavior of grouped large headed studs under UHPC comparing with Normal Strength Concrete (NSC). The push-out experiment was done with studs embedded in the UHPC directly (no shear pockets). The results found higher shear stiffness of about 40% compared with NSC and no visible cracks were observed while using UHPC with large-size studs.

Tawadrous *et al.* [10] described the design system of shear pocket connection in FDPC systems. Hollow Structural Section (HSS) steel confinement was provided for the shear pocket connection. Push-off test

and FEA (ANSYS) were performed to develop design criteria/procedures of HSS formed shear pocket. In many cases, failure modes were found due to studs bending or tearing off combined with the crushing of shear pocket and haunch (if any). FEA gave the predicted yield and ultimate loads comparable to the push-off test with some errors from 2.1–23.9%. The displacements from FEA models ranged from 0.01–0.03 in. and could convert to the non-linear stage. However, some models could achieve only the elastic stage. It was believed that due to the lack of confinement of the concrete surrounding the studs or the sizing of shear pockets was larger than the maximum dimension limit. Similarly, Morcous *et al.* [11] studied the circular shear pocket in FDPC and described the implementation of this system for the construction of the Belden-Laurel bridge project in Nebraska.

Since the study is focusing on the solution for improving the new shear pocket confinement for a cluster of large-size studs, angle ring confinement would be the most efficient solution. The comparative investigation using FEA compared to the push-off test, therefore, was introduced in this study. The analysis includes the studies of model validation (loads, displacement, and failure modes), non-linear concrete behaviors, boundary conditions, and different geometry aspects of angle ring confinement resulting in the stiffness of shear pockets per a finite element analysis approach of ABAQUS based on Mia *et al.* [12] and Fang *et al.* [13]. Once this study was completed, the other modifications, such as using UHPC or HSS shear confinement could be employed in the next phase.

2 Existing Data

2.1 *Tested specimen and geometry*

L-shape FDPC bridge deck panel was tested under the push-off loading condition as shown in Figure 1 to perform composite actions between the concrete deck and the steel girder. The specimen consisted of a full depth concrete deck 600 mm (24 in) wide, 1,100 mm (44 in) long, and 200 mm (8 in) thick with the enlarged loading part about 500 mm (20 in). A cluster of four large-size studs, a diameter of 31.75 mm (1¼ in), and a spacing of 63.5 mm (2½ in) were placed inside the shear pocket of the deck panel. The dimensions of the shear pocket were based on the stud arrangement,
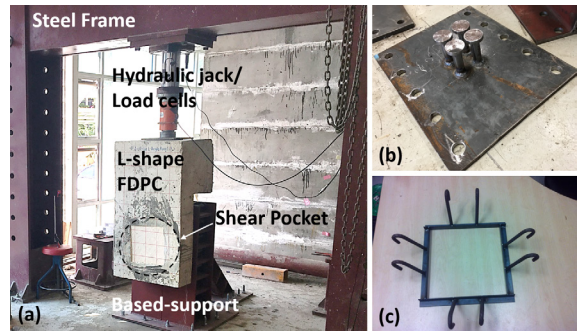

Figure 1: Push-off test set-up: (a) L-shape FDPC attached to a steel frame, (b) A clustered Stud, and (c) L-angle 25 × 25 × 3 mm ring confinement.
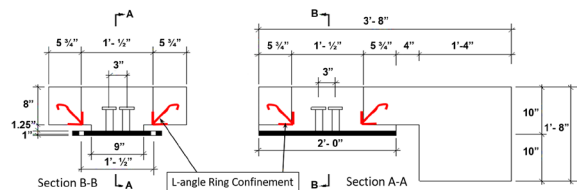

Figure 2: Dimensions of L-shape FDPC deck specimen and layout of a clustered studs and angle ring confinement.

which finalized to a square shape of 300 × 300 mm (12 × 12 in) cut through the thickness of the FDPC deck. The angle ring confinement was assembled from a 25 × 25 × 3 mm L-shape steel angle in a square perimeter around the shear pocket. Two deformed hook bars, 12 mm in diameter, were welded to each side around the perimeter to create extra concrete bonding when cracks. This angle ring confinement was located at the bottom part of the concrete deck around the shear pocket and behaves as a confinement to the clustered large-size studs. Figure 2 shows details of the L-shape FDPC and confinement as aforementioned.

In terms of loading, a hydraulic force was applied to the concrete deck up to the failure points. Loads and displacements were corrected for evaluating shear resistance against various conditions such as with or without confinement, cracks/failure stages, etc. Strain conditions were also observed over the panel, the shear pocket, the studs, and around the confinement.

2.2 *Material properties*

The large-size studs, using SCM440 steel grade based on Thai Industrial Standards (TIS) or equivalent to

grade 1018 steel per Society of Automotive Engineers (SAE) standard, had a tensile strength of 105/130 ksi and yield strength 65/85 ksi. The concrete deck panel was cast with a compressive cylinder strength of 210 ksc and reinforced with DB12 deformed bar grade SD40 (TIS) or equivalent to Grade 60 (AISC) bars. The shear pocket filled in between the concrete deck and clustered studs using high strength mortar with 725 ksc compressive strength. The ring confinement was fabricated using steel angle grade SS540 (TIS) or equivalent A36 (AISC), which had DB12 hook bars grade SD40 attached to all sides of the ring confinement. Table 1 summarizes the material properties used for each part of the specimen.

Table 1: Summary of material properties for push-off

	Type/ Grade	Yield Strength	Ultimate Strength
Grout	Concrete Mortar	725 ksc (10 ksi)	725 ksc (10 ksi)
Concrete	Normal Weight	210 ksc (3 ksi)	210 ksc (3 ksi)
Hook bars	Deform SD40	2400 ksc (34 ksi)	4000 ksc (55 ksi)
Studs	SCM440	4600/6000 ksc (65/85 ksi)	7400/9000 ksc (105/130 ksi)
Angles	SS540	2400 ksc (34 ksi)	4000 ksc (55 ksi)

2.3 *Ring confinement under push-off test*

Under the push-off test of the specimen with the cluster of 4 large-size studs, the angle ring confinement showed the effective transfer of composite actions between the deck and shear pocket up to 44 kg-ton and could sustain the relative displacement up to 45 mm without failure of the studs. This confinement is also well performed among the concrete deck, the shear pocket, and the studs under the service condition, and even better for the ultimate resistant condition as seen from the large relative area of load displacement.

In terms of failure, the crushing of concrete and grout around the bottom layers, between the concrete deck and the steel-based plate, were detected in the loading direction as seen in Figure 3(a). This also resulted in the deterioration of angle ring confinement in the loading direction. However, welding failure at the joints of angles was also observed, which might be considered a local failure of this confinement as shown
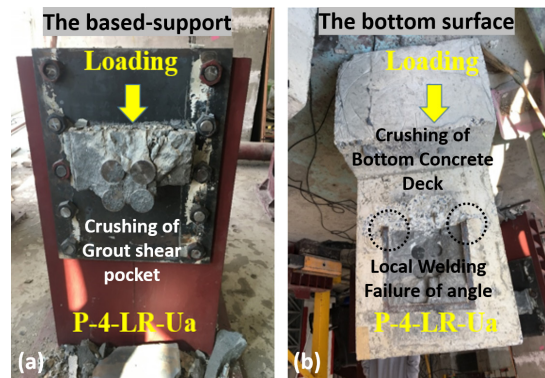

Figure 3: Failures around shear pocket: (a) Crushing of Grout and Concrete deck at the bottom on the loading direction, and (b) Welding failure of angle confinement.

in Figure 3(b). It is believed that this weak point could be eliminated by performing a fully welded length to the angles, and therefore it was not a concern for the comparative study with FEA. Noted, hook bars on the loading direction were eventually torn out apart from the angle confinement when the welding failure occurred.

3 Establishing Finite Element

3.1 *Parts and geometry*

The push-off specimen was finite element modeling using ABAQUS [14] consisting of 5 main parts: FDPC panel, grout, stud connector, angle ring confinement, and hook bars. Noted, reinforcements in concrete were neglected in modeling as not a main concern in this study. The geometries of the FE model were relative to the push-off specimen consisting of 200 mm (8 in) thick FDPC panel with the enlarged thickness of 500 mm (20 in) on the loading area, whereas the width and the length were 600 mm (24 in) and 1,100 mm (44 in), respectively. The grout part with dimensions of 300 × 300 × 225 mm (12 × 12 × 9 in), including a haunch thickness of 25 mm (1 in) was placed inside the shear pocket. Four angles of 25 × 25 × 3 mm were attached together and embedded around the shear pocket's perimeter of 300 × 300 mm at the bottom layer. Two hook bars were constrained to each side of the angle. Lastly, four large-size headed studs were aligned inside the grout part.
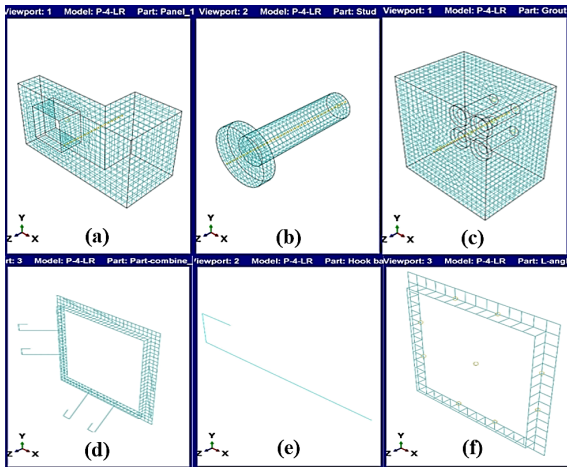
Figure 4: 8-node brick element for (a) Panel, (b) Stud, (c) Grout, (d) Assembled angle confinement with hook bars, (e) 2-node beam element for hook bar, and (f) 4-node plate element for angle ring confinement.

Figure 4 shows meshed models of the five parts where 8-node linear brick element (C3D8R) was used for the L-shape FDPC panel, the individual large-size stud, and the shear pocket part. For the angle ring confinement, 4-node plate elements were assigned to represent the behavior of a thin plate. Lastly, the hook bar was modeled using 2-node beam elements to collate each hook bar to the angle ring confinement correctly as shown in Figure 4(d).

3.2 *Boundary conditions*

Based on the Push-off test, the specimen was attached to the steel frame by connecting the stud inside the shear pocket. Therefore, the fixing condition was applied to the bottom surface of each stud as shown in Figure 5. This applied for all 3-dimensional equilibrium equations: F_x, F_y, F_z, M_x, M_y, and M_z equal to zero. Moreover, the bottom area of the grout part was also controlled from movement in Z-axis to simulate the seating position between the concrete deck and the steel girder below. For the loading condition, the displacement control was provided in this analysis. The maximum movement in the X-axis of 0.5 unit (0.5 in) was applied to the loading area, with the approximate size of the hydraulic jack pushed behind the specimen.

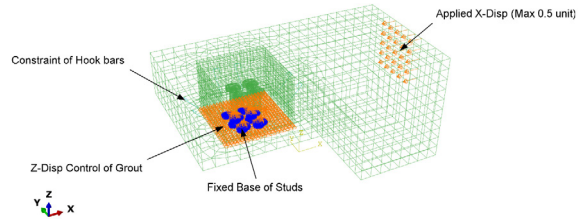In addition, There were some constraints and/or

Figure 5: Boundary conditions to the model: Fixed supports of all 4-stud, Z-displacement control of the grout base, X-displacement for loading condition, and Constraints of hook bars to the panel.

contact conditions assigned to each surface of some parts including: 1) contacts between panel and grout part, 2) contacts between grout and each shear stud part, and 3) constraints by merging and duplicate nodes between L-angle confinement and panel part. These were provided with some certain modes, such as nodal-to-nodal, nodal-to-surface, or surface-to-surface, whichever was applicable to converging the analysis.

3.3 *Material under non-linear properties*

Three material properties were classified herein consisting of: Concrete for panel and grout mortar, Steel presented as angle and deform bars, and Alloy steel SCM440 for studs. Both steel and alloy SCM440 were generally analyzed as bilinear elastoplastic behavior, which could apply both compression and tension phase. However, non-linear plastic models for concrete and grout were more concerned for this study in terms of load resistances, slippages/displacements and the stage of failure that affected the angle ring confinement.

3.3.1 Compressive and tensile strength of concrete

Two non-linear property models for concrete were assigned to FEA using Concrete Damaged (CD) plasticity model and Drucker Prager (DP) plasticity model. These models were provided for both concrete panel and grout shear pocket parts with the compressive strength of 210 ksc (2,987 psi) and 725 ksc (10,312 psi), respectively. On the other hand, the tensile strength equals to the modulus of rupture of concrete (7.5fc') was adopted to the calculation, which had 28.9 ksc (411 psi) for concrete panel and 51.6 ksc (734 psi) psi for grout. Since the strength of concrete was found by
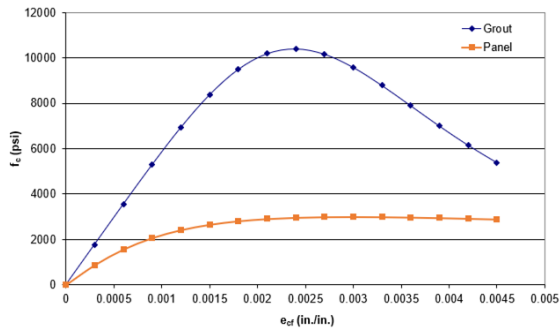
Figure 6: Compressive strength and plastic strain of concrete panel and grout shear pocket.

a uniaxial loading condition, thus Popovic's equations [15] were used for determining equivalent plastic strain and degraded linear unloading stiffness over the compressive and tensile stress-strain relationships. Figure 6 presents the relationship of compressive strength (f_c) and equivalent plastic strain (ε_{cf}) for concrete panel and grout shear pocket assigned to FEA. Since the normal strength concrete was used for the panel, therefore the stress-strain curve of this may flatten compared to the stress-strain curve of the high strength grout. Notes the plastic strain of both concrete constitute models were considered to the longest possible point of 0.0045 in./in. to ensure that the failure of angle confinement could reach in FEA.

Other parameters were also defined to FEA including a dilation angle of 15 degree indicating a prediction of the plastic strain in concrete at each stage, Poisson's ratio of 0.18 for transverse strain in a three-dimensional model, and a viscosity parameter of 1 for a typical plasticity condition.

3.3.2 Behavior of steel

Bilinear compressive and tensile strength of steel were applied to angle confinement, studs, and hook bars. The yield and ultimate stresses of steel angles, hook bars and studs were adopted from the lab test and rounded up for applying the bilinear properties of each steel member in FEA. The plastic properties of steel including yield/ultimate stress and plastic strain were summarized in Table 2, starting from yield stress with zero plastic strain and stepped up to ultimate stress with plastic strain. The modulus of elasticity of 2×10^6 ksc (29,000 ksi) and Poisson's ratio of 0.3 were defined
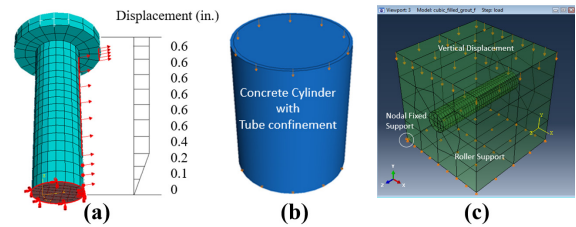

Figure 7: Model validation: (a) Stud under loading condition, (b) Confinement in concrete, and (c) Contact between a single stud and grout.

for the analysis of typical steel members.

Table 2: Summary of plastic properties of steel parts

Plastic/Isotropic	Yield/Ultimate Stress (psi)	Plastic Strain (in/in)
Steel angles and Hook bars	(Y) 40,000	0
	(U) 60,000	0.06
SCM440 Studs	(Y) 92,000	0
	(U) 107,000	0.05

3.4 *Model validation*

Since this research was employed by the high-performance research software "ABAQUS" to the analysis, which the performance and mesh sensitivity tests were included in the validation manual. Therefore, the mesh is discretized in the basic square shape, which not only gives the best and identical results with an isoparametric mapping process but also can be avoided the distortional shape of the element [16].

Therefore, the model validation included three individual necessary cases for observation as shown in Figure 7. The first case is the validity of stud resistance and deformation. The single stud model was fixed at the bottom support, while lateral displacement was applied along the vertical direction. The analysis could result in the maximum resistance of the stud and the relative displacement to this member. The second and third cases included validation of the steel confinement and the contact behavior under closed surfaces such as deck-to-grout and grout-to-stud parts, respectively.

The second case was done by applying vertical displacement to a concrete cylinder model, which was compared against the models with- and without steel tube confinement. The result found that steel confinement could prevent early crack failures and increase stiffness
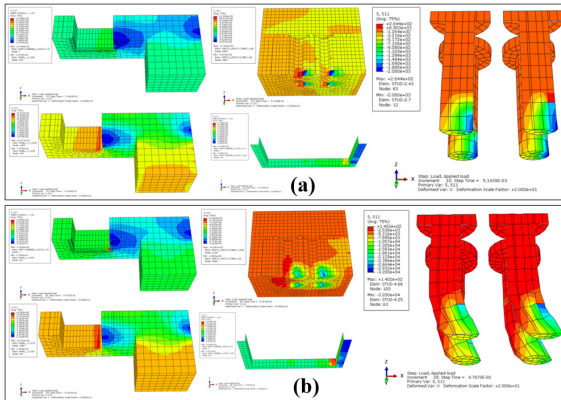
Figure 8: Stress contours S11 (x20 scale factor) in (a) CD model for L5DB12 and (b) DP model for L5DB12.

of the concrete model. Lastly, the contact validity was proved by using a cubic model with a cylindrical part inserted inside. Nodal-to- Surface and Nodal-to-Nodal contact were applicable to this study.

3.5 *Aspects of angle ring confinement*

To clarify the effectiveness of the angle ring confinement, two geometric aspect parameters were considered in the FEA including: thickness of steel angles either 5 or 10 mm, and sizing of hook bars whether DB12 or DB25. Various aspects were swapped between thickness and sizes of hook bars; therefore, 4 FEA models were built consisting of L5DB12, L10DB12, L5DB25, and L10DB25. The nomenclature explains Lx = thickness of angle and DBxx = sizes of deformed hook bars. Noted, the thickness of angles in the model was thicker than that of the experimental specimen to consider the significant effects of the angle confinement to the model and to simply compare against double thickness between 5 and 10 mm as well.

4 Results and Discussion

4.1 *Effects of concrete plasticity model*

Both CD and DP plasticity models gave similar trends in terms of stress concentration contours and deformation shape. However, the DP model could express wider failure patterns whether in the depth of the deck/grout or at the welding corner of the angle confinement. Figure 8 shows longitudinal half-cut
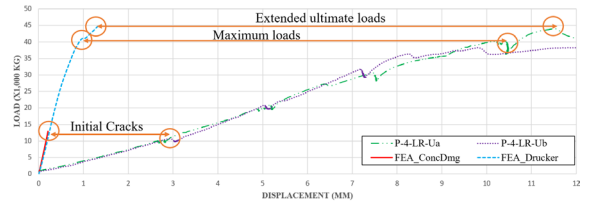

Figure 9: Load-Displacement relations comparing among experimental specimens: P-4-LR-Ua and P-4-LR-Ub; and FE L5DB12 models: CD and DP.

sections of each part (panel, grout, angle, and clustered studs) comparing shear stress contours S11 for CD and DP models. Failure locations can be noticed where high compressive stresses are shown in the blue color.

By comparing the stiffness between the FEA and the experimental specimens in terms of shear resistance vs. displacement, the FE results showed stiffness intensively higher about 10 times than those of the experiment as shown in Figure 9. This occurred in both CD and DP models, but DP model could reach the ultimate resistance up to 45 Ton-force at a 1.5 mm slip. Noted, the high stiffness in FE investigation occurred by controllable factors, such as the precision of the model geometry, the symmetry boundary conditions, the perfection of material distribution, etc. Therefore, this 10 times higher stiffness could be a good comparable number for evaluating and expecting outcomes with push-off, full-scale tests or even in the construction.

The resistance force was calculated by using the average shear stress S11 times the shear surface at the base of the studs. It can be noticed that the largest load point from the DP model could indicate the initial cracking stage of the model, which is beneficial for the forecasting analysis.

4.2 *Effects of angle ring confinement*

The comparative analyses were in two groups of CD and DP models, which are based on the stiffness (load-displacement relationship) for various aspects of the angle confinement. Each group has the FE model with and without angle confinement (ConcDmg_S11 and Drucket_S11), whereas the model with angle confinement had mixed-up aspects among different thicknesses of 5- and 10-mm steel angles and either DB12 or DB25 hook bars.
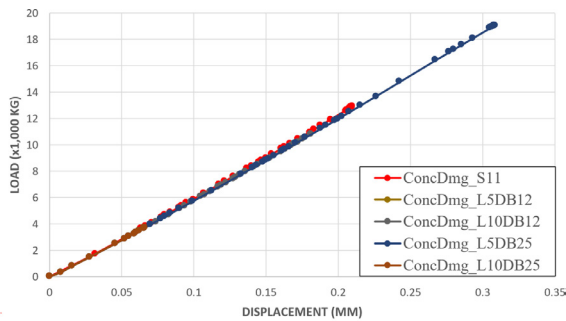
Figure 10: Load-displacement curves among various aspects of angle confinement in CD models.
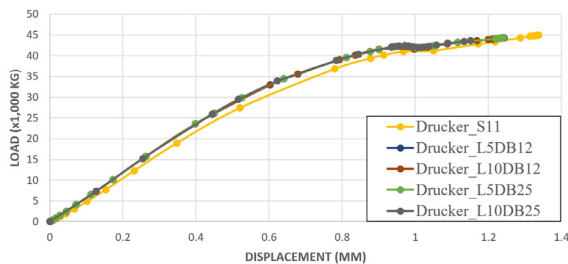

Figure 11: Load-displacement curves among various aspects of angle confinement in DP models.

The group of CD models were presented in Figure 10 as no significant impact could be investigated in any case including the model without confinement. It is believed that CD models were good for an initial crack observation, thus, further analysis using DP models could be better for a more detailed investigation.

Figure 11 expressed the comparative analysis in the DP group, where significant impacts between the model with- and without angle confinement could be identified. Higher stiffness in terms of load resistance is about 6 percent because of shear force against displacement of 42 Ton-force/0.94 mm in model Drucker_L10DB25 vs. 41 Ton-force/0.97 mm in model Drucker_S11. Nonetheless, various aspects of angle confinement showed no major influence on responses to the stiffness or resistance of the entire system. In any case, compatible sizes of angle ring confinement are recommended either using 5 mm thick of angle with DB12 or 10-mm thick of angle with DB25.

4.3 *Failure investigation*

The observation of failure can be seen from S11 stress contours over the different FE parts: panel, grout, and
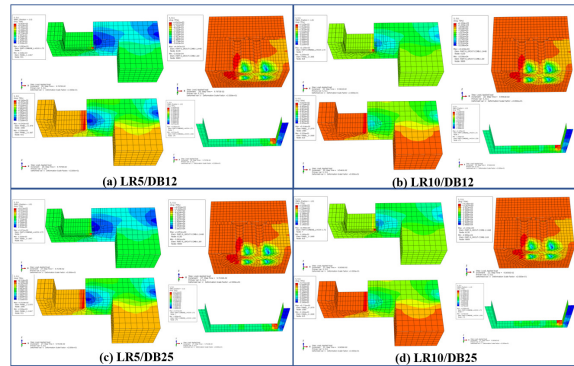

Figure 12: Stress contours S11 (x20 scale factor) in DP models: (a) L5DB12, (b) L10DB12, (c) L5DB25, and (d) L10DB25.

angle ring confinement. The failure of studs was not concerned herein since the specimen was designed to fail around shear pockets either in concrete panel or in grout mortar. Figure 12 presents the stress contours S11 (lateral direction) in the DP models with various aspects of angle confinement, which are used for justifying the failure patterns under the concentrated compressive zones in the blue color. Each figure represents a half-cut section of the panel, the grout, and the angle confinement. It can be noticed that all stress contours are quite in the same patterns. Initial cracks are expected at the bottom shank of the studs on the loading direction up to 25 mm (1 in) above, and then propagate to 10 mm (4 in) half-depth of the panel. At the same time, cracks also occur over the bottom layer of the FDPC panel, which carries on the compressive shear action by the embedded angle confinement on the loading direction. Both areas are expected for initial cracks and eventually become the critical crushing zones propagating around the other nearby areas. On the other hand, cracks due to tension failures could also be detected at the sharp corners both in the shear pocket and in the angle ring confinement as seen from the high tensile stress contour in the red color.

In comparison, the aspects of angle ring confinement show thickness of angles could reduce both compressive and tensile stresses distributed over the confinement itself, but no effect on the grout part. The reduction was roughly 30% on both sides of stresses. This effect of angle aspects was also noticed in the FDPC panel; however, the results were reduced

by about 10% for tensile stresses but increasing about 30% for compressive stresses instead. It is believed that thicker angle confinement gave higher stiffness than the thinner one, and thus resulted in higher resistance sustained in the FDPC panel likewise. In addition, angle aspects in terms of varied sizes of hook bars found unremarkable impact on both the stress contours and/or failure stages.

5 Conclusions

ABAQUS/CAE software was used for finite element investigation comparing to the push-off test of the FDPC system, which consisted of a cluster of large size studs tied with the angle ring confinement around the shear pocket. The FE model validation included the concrete plasticity model, load-displacement of studs, contacting behaviors between interface layers among slab-to-grout and grout-to-studs, interface bonding and boundary conditions of the entire model. Also, the geometric aspects of angle ring confinement were considered in this study to find the most effective shear confinement to the system. The conclusions can be drawn as follows. Non-linear models with Concrete Damage (CD) could identify the initial cracking stage, while Dracker Prager (DP) models could well predict the resistance and stiffness. The FEA results were comparable to those of the push-off whether high stiffness would appear. The initial and propagated crack patterns could be identified by high stress contours in the DP model, which are located at the bottom of the panel and the grout on the loading direction face. By comparing the various geometric aspects of angle ring confinement, the sizes of hook bars did not impact the stiffness but could retain the shear pocket in place. On the other hand, the thickness of the angle increased the stiffness of the system. The tensile and compressive stresses of slab/shear pocket increased up to 10% and 30%, respectively when using thick angles. The suitable geometric aspects of the angle ring confinement were suggested either 5-mm thick angles with DB12 hook bars or 10-mm thick angles with DB25 hook bars. It was believed that the final non-linear FEA model was reliable for future comparative studies to various FDPC push-off specimens with different confinement configurations, material properties, geometries for slab, studs, and/or shear pocket.

Author Contributions

K.S.: conceptualization, methodology, research design, data analysis, investigation, writing-original draft, funding acquisition and project administration. S.P., C.B., K.R., N.C: writing-reviewing and editing. All authors have read and agreed to the published version of the manuscript.

Conflicts of Interest

The authors declare no conflict of interest, no known competing financial interests or personal relationships that could have appeared to influence the work reported in this paper.

References

[1] T. Yamane, M. K. Tadros, S. S. Badie, and M. C. Baishya, "Full-depth precast prestressed concrete bridge deck system," *Prestressed/Precast Concrete Institute (PCI) Journal*, vol. 43, no. 3, pp. 50–66, 1998.

[2] The American Association of State Highway and Transportation Officials (AASHTO), *AASHTO LRFD Bridge Design Specifications*, 6th ed. Washington, DC: AASHTO, 2012.

[3] S. S. Badie, M. K. Tadros, H. K. Kakish, D. L. Splittgerber, and M. C. Baishya, "Large studs for composite action in steel bridge girders," *Journal of Bridge Engineering*, vol. 7, no. 3, pp. 195–203, 2002.

[4] S. S. Badie, A. F. M. Girgis, M. K. Tadros, and K. Sriboonma, "Full-scale testing for composite slab/beam systems made with extended stud spacing," *Journal of Bridge Engineering*, vol. 16, no. 5, pp. 653–661, 2011.

[5] K. Sriboonma and S. S. Badie, "Practical steel

confinements for wildly spaced clustered large stud shear connectors in composite bridge deck panel systems," in *2010 Structures Congress*, pp. 3216–3227, 2010.

[6]   K. Sriboonma and S. Pornpeerakeat, "Experimental investigation of steel confinement of clustered large-size stud shear connector in full-depth precast bridge deck panel," *Key Engineering Materials*, vol. 856, pp. 99–105, Aug. 2020.

[7]   K. Sriboonma, "Fatigue behavior of steel ring confinement for a clustered stud shear connector in full-depth precast concrete bridge deck panel," *Materials Today: Proceedings*, vol. 52, pp. 2555–2561, Jan. 2022.

[8]   S. Fang, S. Zhang, Z. Cao, G. Zhao, Z. Fang, Y. Ma, H. Jiang, "Effects of stud aspect ratio and cover thickness on push-out performance of thin full-depth precast UHPC slabs with grouped short studs: Experimental Evaluation and Design Consideration," *Journal of Building Engineering*, vol. 67, May 2023, Art. no. 105910.

[9]   J. Wang, Q. Xu, Y. Yao, J. Qi, and H. Xiu, "Static behavior of grouped large headed stud-UHPC shear connectors in composite structures," *Composite Structures*, vol. 206, pp. 202–214, Dec. 2018.

[10] R. Tawadrous and G. Morcous, "Design of shear pocket connection in full-depth precast concrete deck systems," *Engineering Structure*, vol. 179, pp. 367–386, Jan. 2019.

[11] G. Morcous and R. Tawadrous, "Circular shear pocket connection for full-depth precast concrete deck construction," *Journal of Bridge Engineering*, vol. 26, no. 5, May 2021, Art. no. 04021019.

[12] M. M. Mia and A. K. Bhowmick, "A finite element based approach for fatigue life prediction of headed shear studs," *Structures*, vol. 19, pp. 161–172, Jun. 2019.

[13] J. Qi, J. Wang, M. Li, and L. Chen, "Shear capacity of stud shear connectors with initial damage experiment, FEM model and theoretical formulation," *Steel and Composite Structures*, vol. 25, no. 1, pp. 79–92, Sep. 2017.

[14] *ABAQUS Analysis User's Manual, Version 6.13*, Dassault Systemes Simulia, Inc., Providence, RI, USA, 2013.

[15] S. Popovics, "A numerical approach to the complete stress strain curve for concrete," *Cement and Concrete Research*, vol. 3, no. 5, pp. 583–599, Sep. 1973.

[16] T. H. H. Pian and K. Sumihara, "Rational approach for assumed stress finite elements," *International Journal for Numerical Methods in Engineering*, vol. 20, no. 9, pp. 1685–1695, Sep. 1984.